2014

Membrane Efficiency of a Dense Prehydrated GCL

Michael A. Malusis
mam028@bucknell.edu

Akmal Daniyarov

Membrane Efficiency of a Dense, Prehydrated GCL

M.A. Malusis[1] and A.S. Daniyarov[2]

[1]*Associate Professor, Department of Civil and Environmental Engineering, Bucknell University, Lewisburg Pennsylvania 17837, USA; PH +01 1 570 577 1683; email: michael.malusis@bucknell.edu*

[2]*Graduate Student, Department of Civil and Environmental Engineering, Bucknell University, Lewisburg Pennsylvania 17837, USA; PH +01 1 570 577 1112; email: asd007@bucknell.edu*

ABSTRACT

The purpose of this study was to investigate the membrane efficiency of a dense, prehydrated geosynthetic clay liner (DPH-GCL) in the presence of monovalent salt (KCl) solutions. Membrane efficiency coefficients, ω, were determined for 5-mm-thick DPH-GCL specimens subjected to three different source KCl solutions (source concentration, C_o = 8.7, 20 and 47 mM) in rigid-wall diffusion cells under no-flow conditions. The source KCl solutions and de-ionized water (DIW) were circulated across the top and bottom specimen boundaries, respectively, and values of ω were determined based on the differential pressure induced across the specimens due to prevention of chemico-osmotic liquid flux. The DPH-GCL specimens exhibited the same trend of decreasing ω with increasing C_o as conventional granular GCL specimens tested in previous studies. However, the DPH-GCL specimens exhibited higher ω relative to conventional GCL specimens tested at the same source KCl concentration. These findings are consistent with the lower hydraulic conductivities, k, measured for the DPH-GCL specimens and are attributed primarily to the higher dry density of the DPH-GCL specimens (~1.1 Mg/m^3) relative to the conventional GCL specimens (~0.4 Mg/m^3), although differences in bentonite texture (i.e., powdered bentonite in the DPH-GCL versus granular bentonite in the conventional GCL) and chemical treatment of the bentonite in the DPH-GCL (via the prehydration solution) also may have contributed to higher ω for the DPH-GCL.

Keywords: Bentonite; Geosynthetic Clay Liners; Membrane Efficiency

1 INTRODUCTION

The potential for engineered soil and geosynthetic barriers containing sodium bentonite to act as semipermeable membranes, restricting the passage of ions while allowing relatively unrestricted flow of water, has been well documented in studies conducted over the past decade (e.g., Malusis and Shackelford 2002a,b; Yeo et al. 2005; Henning et al. 2006; Kang and Shackelford 2010, 2011; Mazzieri et al. 2010; Shackelford 2013). The results of these studies indicate that, among the different types of bentonite-rich barriers used in geoenvironmental containment applications, geosynthetic clay liners (GCLs) are most likely to exhibit significant membrane behavior (i.e., high membrane efficiency) due to the high bentonite content (~100 %) in these barriers. Such behavior can improve the containment performance of a GCL by limiting the migration of solutes through the GCL due to hyperfiltration, chemico-osmosis, and restricted diffusion (Malusis et al. 2003).

The vast majority of studies conducted to investigate the membrane behavior of GCLs have been performed on conventional GCL specimens consisting of loose, granular bentonite held between two geotextiles (e.g., by stitching or needle-punching), such as the Bentomat® DN GCL shown in Fig. 1a (see Malusis and Shackelford 2002a,b; Shackelford and Lee 2003; Kang and Shackelford 2011). However, a relatively new GCL product known as a dense, prehydrated GCL (DPH-GCL; see Fig. 1b) has emerged as a potentially attractive alternative to conventional GCLs. Whereas conventional GCLs are typically ~10 mm thick and contain naturally dry (non-prehydrated) granular bentonite, the DPH-GCL in Fig. 1b is 5-7 mm thick and contains a 4-6 mm calendered layer of powdered bentonite that has been factory prehydrated with a treatment solution designed to improve the flexibility and resilience of the bentonite (Di Emidio 2010). The combination of the smaller manufactured thickness and the higher bentonite mass per unit area (i.e., ~5 kg/m^2 for the DPH-GCL versus ~4 kg/m^2 for the conventional GCL) yields a considerably higher as-received dry density for the DPH-GCL (~1.1 Mg/m^3) relative to a conventional GCL (~0.4 Mg/m^3). As a result, the DPH-GCL exhibits extremely low hydraulic conductivities, k, to water (1×10^{-12} to 4×10^{-12} m/s; e.g., see Kolstad et al. 2004), approximately an order of magnitude lower than a conventional GCL. Also, DPH-GCL specimens have been shown to exhibit little or no degradation in k when permeated with highly concentrated salt solutions (Kolstad et al. 2004; Katsumi et al. 2008).

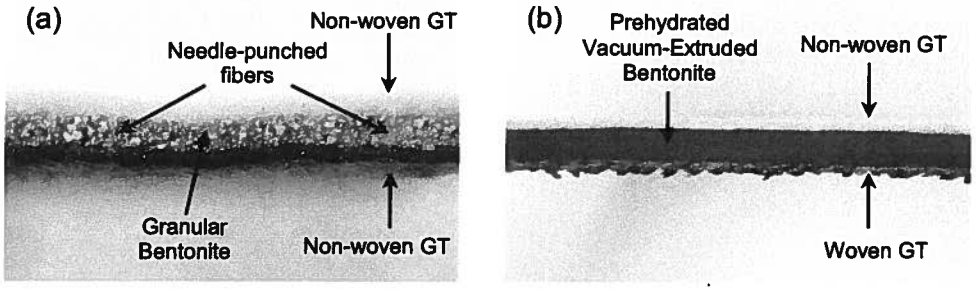

Figure 1. Photographs of GCL cross sections: (a) conventional GCL (Bentomat® DN); (b) DPH-GCL.

Quantitatively, membrane behavior is expressed in terms of a membrane efficiency coefficient, ω, which ranges from zero to unity ($0 \leq \omega \leq 1$). An ideal membrane ($\omega = 1$) would not allow any ions to enter the pores, whereas a non-membrane ($\omega = 0$) would not restrict ion transport. In general, GCLs act as non-ideal membranes, with ω varying over $0 < \omega < 1$ depending on factors such as the dry density (or porosity), applied stress, and the types and concentrations of ions attempting to pass through the pores (e.g., Malusis and Shackelford 2002a,b; Shackelford and Lee 2003; Kang and Shackelford 2011) Given the higher dry density of the bentonite in a DPH-GCL, higher values of ω may be expected for DPH-GCLs relative to conventional GCLs tested under similar conditions. However, only one value of ω has been reported in the literature for a DPH-GCL specimen (Di Emidio 2010). Thus, the purpose of this study was to perform membrane tests on DPH-GCL specimens using monovalent salt (KCl) solutions over a range of concentrations (i.e., 8.7 – 47 mM) to facilitate comparison with conventional GCL specimens tested previously by Malusis and Shackelford (2002a) and Kang and Shackelford (2011).

2 MATERIALS AND METHODS

2.1 DPH-GCL

The DPH-GCL being tested in this study, shown in Fig. 1b, is manufactured by Rawell Environmental Ltd. (Hoylake, UK) and is commercially available under the trade name Rawmat® HDB. This DPH-GCL is fabricated by blending natural Na bentonite with a dilute solution containing carboxymethyl cellulose (CMC) and sodium polyacrylate (SPA) in a high speed mixer, and then extruding the bentonite under vacuum into a thin, dense sheet (Flynn and Carter 1998; Di Emidio 2010). The large polymer (CMC and SPA) molecules are believed to enhance the chemical resistance of the bentonite by bonding with the Na ions in the bentonite interlayers to promote osmotic swell upon exposure to electrolyte solutions (Flynn and Carter 1998; Kolstad et al. 2004; Di Emidio 2010).

The DPH-GCL sheets acquired for this study measured 4.9-5.6 mm in thickness excluding the geotextiles (1.0-1.5 mm), and the average dry bentonite mass per original unit area (i.e., area prior to drying) was determined to be 4.88 kg/m^2 based on seven replicate measurements. A specific gravity, G_s, of 2.69, was measured for the bentonite following the procedure given by ASTM D 854-10. Based on these values, the average porosity and dry density of the as-received DPH-GCL sheets were estimated to be 0.59 and 1.1 Mg/m^3, respectively. Initial degrees of saturation averaged 88 %, indicating that the sheets were well hydrated but not fully hydrated in the as-received condition. As reported by Di Emidio (2010), the bentonite exhibits a cation exchange capacity of 52 meq/100 g (52 $cmol_c$/kg) and contains primarily sodium ions (~78 %) on the exchange complex.

2.2 Liquids

The liquids used in this study include de-ionized water (DIW; electrical conductivity, *EC* = 4 mS/m) and 8.7, 20, and 47 mM KCl (certified A.C.S., Fisher Scientific, Rochester, NY) solutions prepared using DIW. The KCl concentrations were chosen to be the same as those used by Malusis and Shackelford (2002a) and Kang and Shackelford (2011) in membrane tests on conventional GCL (Bentomat® DN) specimens. In some of the tests, the DIW and KCl solutions were amended with 500 ppm of DOWICIL® QK-20 biocide (Dow Chemical Company, Midland, MI) to minimize potential gas generation in the DPH-GCL due to biological activity (see Jo et al. 2005; Di Emidio et al. 2008). Jo et al. (2005)

notes that 500 ppm Dowicil QK-20 is effective for controlling microbial activity without significantly altering the clay fabric.

2.3 Specimen Preparation and Testing

Circular specimens (diameter = 71 mm) of the DPH-GCL were cut from larger sheets, and the lower woven geotextile (see Fig. 1) was removed and replaced with a separate piece of the upper non-woven geotextile. The specimens then were placed inside of rigid-wall testing apparatus consisting of an acrylic cylinder with a base pedestal and top piston that encloses the specimen between two porous stones, as depicted in Figure 2. The top piston is fixed in place to prevent swelling, thereby maintaining a constant specimen thickness. Prior to membrane testing, the specimens were permeated with DIW to further hydrate and saturate the specimens and to measure the baseline hydraulic conductivity to water (k_w). However, there was no attempt to flush the soluble salts from the specimens, as has been done in several previous studies on membrane behavior of GCLs (e.g., Malusis and Shackelford 2002a,b; Kang and Shackelford 2009, 2011; Di Emidio 2010). For example, the DPH-GCL specimen tested by Di Emidio (2010) was permeated with DIW for 3.8 years (17 pore volumes of flow [PVF]) to remove most of the soluble salts prior to testing for membrane efficiency. In contrast, the specimens in this study were permeated for 4-6 months (~2 PVF). Thus, the overall test durations in this study were much shorter, and the specimens were considered to be a better representation of typical field conditions.

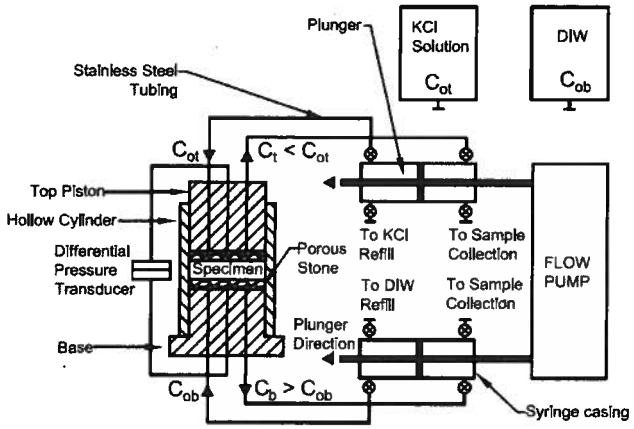

Figure 2. Schematic diagram of testing apparatus (redrawn after Malusis and Shackelford 2002a).

Three membrane tests were conducted in this study. Each test was performed on a separate DPH-GCL specimen and utilized a different source KCl concentration (C_{ot} = 8.7, 20, or 47 mM). Each test was performed using the apparatus illustrated in Figure 2, in general accordance with the procedures described by Malusis and Shackelford (2002a). A syringe pump was used to continuously circulate DIW or a KCl solution across the top and bottom specimen boundaries at a rate of 4.8×10^{-10} m^3/s to establish a solute concentration difference across the specimen while maintaining a closed system (i.e., no volumetric flux of liquid could occur across the specimen during the tests). To determine the membrane efficiency, DIW was circulated across the bottom boundary, whereas the KCl solution was circulated across the top boundary. The resulting concentration difference induced a pressure difference across the specimen (i.e., due to prevention of chemico-osmotic liquid flux through the specimen), which was measured at 15-minute intervals using a differential pressure transducer. Values of the membrane efficiency coefficient, ω, were determined using the following equation (Malusis et al. 2001):

$$\omega = \Delta P / \Delta \pi \tag{1}$$

where ΔP is the induced differential pressure and $\Delta \pi$ is the theoretical chemico-osmotic pressure difference for an "ideal" membrane (ω = 1). Values of $\Delta \pi$ were computed from the applied KCl concentration difference (ΔC) using the van't Hoff equation (Katchalsky and Curran 1965), or

$$\Delta \pi = \nu R T \Delta C \tag{2}$$

where ν is the number of ions per molecule of salt (ν = 2 for KCl), R is the universal gas constant (8.314 J $mol^{-1}K^{-1}$), and T is absolute temperature (K). The van't Hoff equation is based on the assumption that the electrolyte solutions are ideal and dilute and, thus, is an approximation of the true chemico-osmotic pressure. According to Fritz (1986), the approximation error is small (<5%) for monovalent salt (e.g., NaCl, KCl) concentrations <1 M. The tests were conducted at an average ambient temperature of 22 °C (295 K).

Although the circulation rate of 4.8×10^{-10} m^3/s was sufficient to establish a reasonably constant KCl concentration difference across the specimens, diffusion of KCl through the specimen (i.e., from top to bottom) resulted in small but measurable differences between the inflow concentrations (C_{ot} and C_{ob}) and outflow concentrations (C_t and C_b) in the circulation loops at the specimen boundaries (i.e., $C_t < C_{ot}$ and $C_b > C_{ob}$; see Fig. 2). Also, since sodium was the predominant soluble salt species and the predominant exchangeable cation species in the DPH-GCL bentonite (Di Emidio 2010), the specimens were expected to elute appreciable concentrations of sodium ions (Na^+) during the tests. Therefore, the outflow solutions from each specimen boundary were collected and analyzed for electrical conductivity (EC) and for K^+, Na^+, and Cl^- concentrations using ion chromatography. Other cation and anion species also were monitored (e.g., Ca^{2+}, Mg^{2+}, SO_4^{2-}, etc.), but the concentrations of these species were minor relative to K^+, Na^+, and Cl^-.

The membrane tests were carried out until the transport of both K^+ and Cl^- into the bottom boundary approached steady-state conditions (i.e., ion exchange of K^+ in the specimens was essentially complete). The specimens were then permeated with the source KCl solution (the same source solution used in the membrane test) to determine the final hydraulic conductivity, k_c.

3 RESULTS AND DISCUSSION

3.1 Induced Differential Pressures

The differential pressures ($-\Delta P$) measured in the tests are presented in Figure 3. At the start of each test, DIW was circulated across both the bottom and top boundaries to establish a baseline differential pressure, $-\Delta P_o$, across the specimen. Despite the absence of an applied concentration difference during this stage, non-zero values of $-\Delta P_o$ are possible due, at least in part, to slight differences in hydraulic conductivity of the porous stones at the specimen boundaries (e.g., see Malusis et al. 2001). In this study, values of $-\Delta P_o$ = 0.7, 1.7, and 1.7 kPa were measured in the three tests (see Fig. 3). After introduction of the KCl solution at the top boundary, $-\Delta P$ increased rapidly and eventually approached a steady value over time (the daily variations in $-\Delta P$ illustrated in Fig. 3 result from temporary release of some of the pressure during the daily process of refilling the syringes). The differential pressures at steady state, $-\Delta P_{ss}$, increased with increasing C_{ot} and were estimated to be 31.7, 53.5 and 56.5 kPa. Thus, the net (effective) differential pressures attributed to membrane behavior, $-\Delta P_e$ (= $-\Delta P_{ss} + \Delta P_o$), were 30, 52.8 and 54.8 kPa, respectively (see Fig. 3). Although the trends of $-\Delta P$ over time were similar in each test, the trend was more erratic throughout much of the test conducted using the 8.7 mM KCl solution (Fig. 3a), which did not contain the biocide. Because the suspected cause of the erratic behavior was gas generation by microbial activity in the specimens, biocide was added to both the DIW and the 20 mM and 47 mM solutions for the tests in Figures. 3b-c. The $-\Delta P$ trends in these tests were more consistent over time, indicating that microbial activity may have been responsible for the more erratic behavior illustrated in Figure 3a.

3.2 Membrane Efficiency Coefficients

Membrane efficiency coefficients, ω, for each of the three specimens (based on the steady-state $-\Delta P_e$ values in Figure 3) are presented in Table 1. The values designated ω_o represent membrane efficiency coefficients computed based on the input (source) KCl concentrations introduced at the specimen boundaries, i.e., $\Delta C = C_{ot} - C_{ob}$ in Eq. 2. Because DIW was used as the source solution at the bottom boundary, $C_{ob} = 0$. Thus, Eq. 2 reduces to the following:

$$\Delta\pi_o = -2RTC_{ot} \tag{3}$$

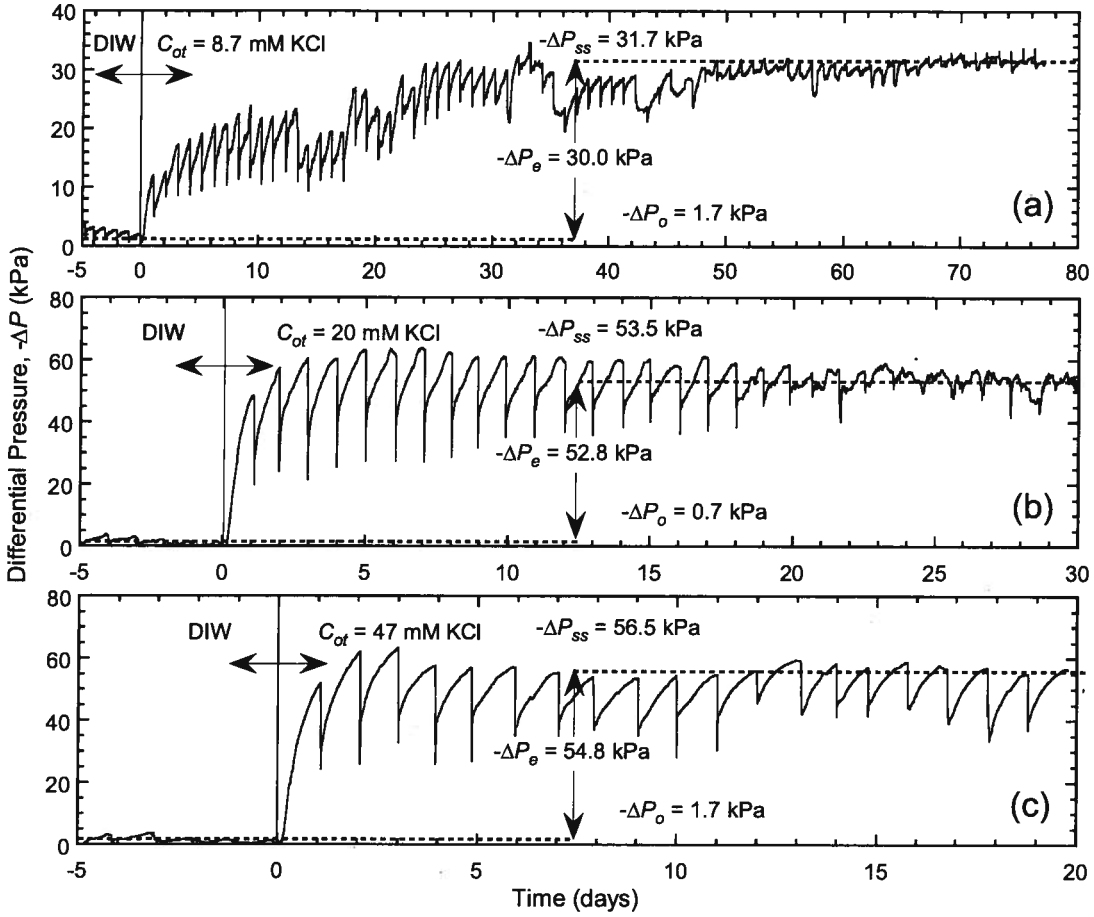

Figure 3. Chemico-osmotic induced differential pressures across DPH-GCL specimens: (a) C_{ot} = 8.7 mM KCl; (b) C_{ot} = 20 mM KCl; (c) C_{ot} = 47 mM KCl. Note: 500 ppm biocide was added to the DIW and the 20 mM and 47 mM KCl solutions for the tests illustrated in (b) and (c).

Table 1. Summary of membrane test results.

	Test conditions			Membrane test results (values at steady state)					Hydraulic conductivities
Test No.	C_{ot} (mM)	L (mm)	n (---)	$-\Delta P_e$ (kPa)	$-\Delta\pi_o$ (kPa)	$-\Delta\pi_{av}$ (kPa)	$\omega_o = \Delta P_e / \Delta\pi_o$	$\omega_{av} = \Delta P_e / \Delta\pi_{av}$	k_w, k_c ($\times 10^{-12}$ m/s)
1	8.7	5.2	0.53	30	42.6	40.9	0.70	0.73	1.4, 1.8
2	20	5.6	0.64	52.8	98.0	92.0	0.54	0.57	1.1, 1.3
3	47	5.0	0.60	54.8	230	212	0.24	0.26	2.0, 1.9

C_{ot} = source KCl concentration, L = specimen thickness, n = porosity, ΔP_e = net (effective) differential pressure, $\Delta\pi_o$ = chemico-osmotic pressure difference based on input (source) concentrations at specimen boundaries, $\Delta\pi_{av}$ = chemico-osmotic pressure difference based on average concentrations at specimen boundaries, ω = membrane efficiency coefficient, k_w = hydraulic conductivity to water (measured prior to testing), k_c = hydraulic conductivity to source KCl solution (measured after testing).

Thus, Eq. 3 is based on the assumption of "perfectly flushing" boundary conditions in which the boundary concentrations are maintained at C_{ot} = 8.7, 20, or 47 mM and C_{ob} = 0. However, as discussed previously, diffusion of KCl through the specimen resulted in a loss of KCl mass from the top boundary and a gain in KCl mass at the bottom boundary, such that $C_t < C_{ot}$ and $C_b > 0$. These slight deviations from the "perfectly flushing" conditions are illustrated in Figure 4 for the test conducted with the 47 mM KCl solution. In this case, the K^+ and Cl^- concentrations exiting the top

boundary (C_t) and bottom boundary (C_b) converged to approximately 43 mM and 3.4 mM, respectively, at the end of the test.

Because the boundaries were not perfectly flushed, more accurate values of ω were determined based on average boundary concentrations. These concentrations were computed as the arithmetic averages between the input (source) and exit boundary concentrations, as follows:

$$C_{t,av} = (C_{ot} + C_t)/2 \; ; \quad C_{b,av} = C_b/2 \tag{4}$$

Also, the chemico-osmotic pressure differences based on the average boundary concentrations, $\Delta\pi_{av}$, were computed as follows based on Eq. 2:

$$\Delta\pi_{av} = 2RT(C_{b,av} - C_{t,av})_{ss} \tag{5}$$

where the subscript "ss" represents steady state. Values of ω computed using $\Delta\pi = \Delta\pi_{av}$ (designated as ω_{av} in Table 1) are slightly higher than ω_o, because $\Delta\pi_{av}$ is slightly lower than $\Delta\pi_o$. However, the differences between ω_{av} and ω_o are small (<8 %).

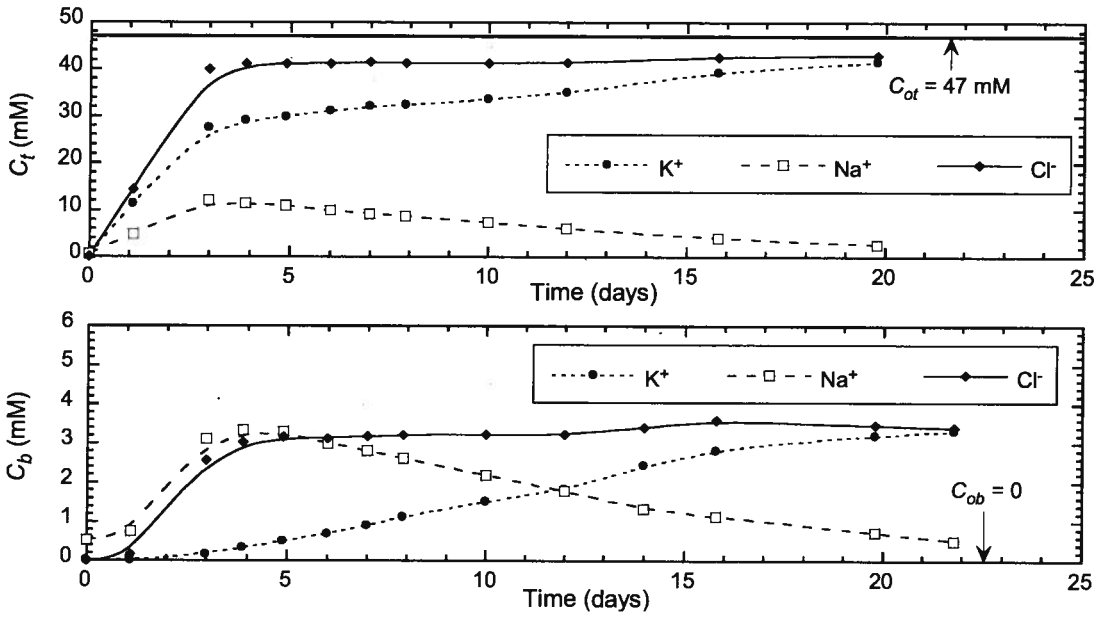

Figure 4. Ion concentration at top (C_t) and bottom (C_b) specimen boundary for membrane efficiency test with 47 mM KCl

The results in Figure 4 also illustrate that steady diffusion of Cl^- through the specimens was achieved long before steady transport was approached for K^+, as was expected based on the greater reactivity of the K^+ with the bentonite. In this case, C_t and C_b for Cl^- became reasonably steady after ~5 days of testing. In contrast, ~21 days of testing was needed for ion exchange (K^+ for primarily Na^+) to reach completion, such that the C_t and C_b for K^+ approached those of Cl^- and the C_t and C_b for Na^+ were lower than those measured at $t = 0$. Although at least some of the Na^+ released at the top and bottom boundaries was initially present in the specimen pores as soluble salts (as indicated by the non-zero boundary concentrations of Na^+ at $t = 0$), the increase and subsequent decrease in the boundary Na^+ concentrations over time illustrate that the Na^+ trends in Figure 4 were governed primarily by the release of exchangeable Na^+.

3.3 COMPARISON TO CONVENTIONAL GCLs

The ω_{av} values in Table 1 are plotted as a function of source KCl concentration (C_{ot}) in Figure 5, along with those reported previously for the Bentomat® DN conventional GCL by Malusis and Shackelford

(2002a) and Kang and Shackelford (2011). The results show that ω_{av} decreases with increasing source concentration for both the conventional GCL and the DPH-GCL. These trends are consistent with expected behavior for bentonite based on DDL theory (Kemper and Rollins 1966; Shackelford et al. 2000; Malusis and Shackelford 2002a,b) and suggest that the presence of the polymers in the DPH-GCL did not prevent DDL shrinkage upon exposure to the KCl solutions, even though the hydraulic conductivities to the KCl solutions (measured after testing) were nearly the same as the hydraulic conductivities to DIW (measured before testing; see Table 1). Nonetheless, the DPH-GCL specimens exhibited higher ω for a given source concentration relative to the conventional GCL specimens. The higher ω values for the DPH-GCL specimens are attributed primarily to the lower porosity (or higher dry density) of these specimens. However, the ω values for the conventional GCL compressed to porosities approaching those of the DPH-GCL specimens (i.e., n = 0.66-0.70) are still appreciably lower than ω for the DPH-GCL specimens, indicating that factors other than porosity may be contributing to the differences in ω. For example, it is possible that the presence of the CMC and SPA in the DPH-GCL provided some benefit in terms of reducing DDL shrinkage. Also, the DPH-GCL was fabricated using powdered bentonite, whereas the conventional GCL contained granular bentonite. As noted by Malusis and Shackelford (2002a), the coarse granules in a conventional GCL may contribute to larger pore sizes and, thus, lower membrane efficiencies relative to powdered bentonite specimens. Finally, the tests by Kang and Shackelford (2011) were conducted in flexible wall cells, whereas the tests in this study were conducted in rigid wall cells. Additional research is needed to further investigate the impacts of these differences on membrane efficiency.

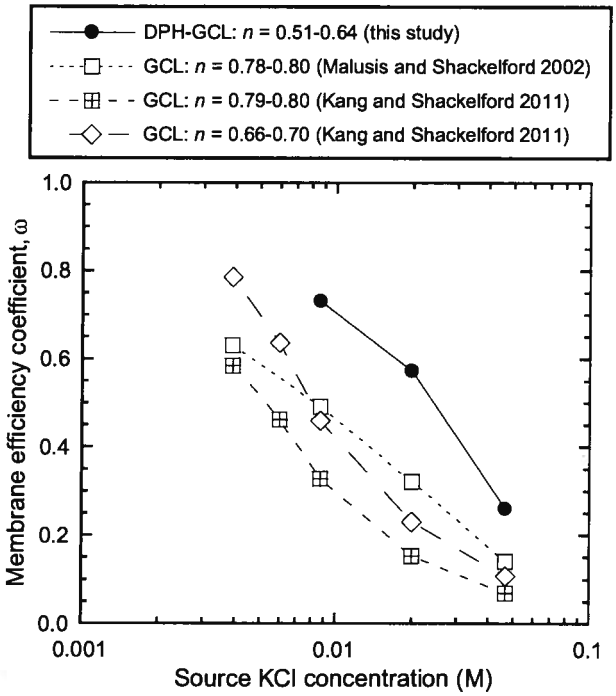

Figure 5. Membrane efficiency as function of source KCl concentration (C_{ot}) for DPH-GCL specimens and conventional (Bentomat® DN) GCL specimens.

4 CONCLUSIONS

This study reports the results of an experimental investigation conducted to determine the membrane efficiency coefficients (ω) for DPH-GCL specimens subjected to potassium chloride (KCl) solutions with source concentrations of 8.7, 20 and 47 mM. Values of ω for the DPH-GCL specimens decreased with increasing KCl concentration, as expected based on diffuse double layer theory, despite any potential mitigation of diffuse double layer shrinkage that may have been provided by the polymeric treatment agents added to the DPH-GCL bentonite via the prehydration solution. Nonetheless, the ω values for the DPH-GCL specimens were shown to be greater (for a given source KCL concentration)

relative to those for conventional GCL specimens containing non-prehydrated Na bentonite granules. The superior membrane efficiencies of the DPH-GCL specimens relative to the conventional GCL specimens are attributed primarily to the higher dry density (lower porosity) of the specimens, although differences in bentonite texture (i.e., powdered bentonite in the DPH-GCL versus granular bentonite in the conventional GCL) and chemical treatment of the bentonite in the DPH-GCL also may have contributed to higher ω for the DPH-GCL. Additional research is needed to elucidate the relative significance of these different potential factors.

5 ACKNOWLEDGMENTS

Financial support for this research was provided by Bucknell University. The authors thank Rawell Environmental Ltd. for providing the DPH-GCL samples tested in this study. Also, the authors gratefully acknowledge Huan Luong, Steven Beightol, James Gutelius, Melissa Replogle, and Minwoo Cho for their assistance with this work.

6 REFERENCES

Di Emidio, G. (2010). Hydraulic and chemico-osmotic performance of polymer treated clays. *Ph.D. Dissertation*, Ghent University, Belgium.

Di Emidio, G., Mazzieri, F, and van Impe, W. F. (2008). Hydraulic conductivity of a dense prehydrated GCL: Impact of free swell and swelling pressure. *Proceedings of the 4th European Geosynthetics Conference.* Paper 320 (CD-ROM), 7 p.

Flynn, B. N. and Carter, G. C. (1998). Waterproofing material and method of fabrication thereof. U.S. patent No. 6,537,676 B1.

Fritz, S. J. (1986). Ideality of clay membranes in osmotic processes: A review. *Clays and Clay Minerals*, 34(2), 214-223.

Henning, J., Evans, J., and Shackelford, C. (2006). Membrane Behavior of Two Backfills from Field-Constructed Soil-Bentonite Cutoff Walls. *Journal of Geotechnical and Geoenvironmental Engineering,* 132(10), 1243–1249.

Jo, H. Y., Benson, C. H., Shackelford, C. D., Lee, J. -M. and Edil, T. B. (2005). Long-term hydraulic conductivity of a geosynthetic clay liner permeated with inorganic salt solutions., *Journal of Geotechnical and Geoenvironmental Engineering, ASCE* 131 (4), 405-417

Kang, J. B., and Shackelford, C. D. (2010). Membrane behavior of compacted clay liners. *Journal of Geotechnical and Geoenvironmental Engineering,* 136, 10, 1368-1382.

Kang, J. B., and Shackelford, C. D. (2011). Consolidation enhanced membrane behavior of a geosynthetic clay liner. *Geotextiles and Geomembranes*, 29, 6, 544-556.

Katsumi, T., Ishimori, H., Fukagawa, R., and Onikata, M. (2008). Long-term barrier performance of modified bentonite materials against sodium and calcium permeant solutions. *Geotextiles and Geomembranes*, 26, 1, 14-30.

Katchalsky, A., and Curran, P. F. (1965). *Nonequilibrium thermodynamics in biophysics.* Cambridge: Harvard University Press.

Kemper, W. D., and Rollins, J. B (1966). Osmotic efficiency coefficients across compacted clays. *Soil Science Society of America Proceedings,* 30(5), 529-534.

Kemper, W. D. and Quirk, J. P. (1972). Ion mobilities and electric charge of external clay surfaces inferred from potential differences and osmotic flow. *Soil Science Society of America Proceedings*, 36, 426-433.

Kolstad, D. C., Benson, C. H., and Edil, T. B. (2004). Hydraulic conductivity and swell of nonprehydrated geosynthetic clay liners permeated with multispecies inorganic solutions. *Journal of Geotechnical and Geoenvironmental Engineering,* 130, 12, 1236-1249.

Malusis, M. A., Shackelford, C. D., and Olsen, H. W. (2001). A laboratory apparatus to measure chemico-osmotic efficiency coefficients for clay soils. *Geotechnical Testing Journal*, 24, 229-242.

Malusis, M. A. and Shackelford, C. D. (2002a). Chemico-osmotic efficiency of a geosynthetic clay liner. *Journal of Geotechnical and Geoenvironmental Engineering,* 128(2), 97-106.

Malusis, M. A. and Shackelford, C. D. (2002b). Coupling effects during steady-state solute diffusion through a semipermeable clay membrane. *Environmental Science and Technology*, 36(6), 1312-1319.

Malusis, M. A., Shackelford, C. D., and Olsen, H. W. (2003). Flow and transport through clay membrane barriers. *Engineering Geology,* 70(2-3), 235-248.

Mazzieri, F., Di Emidio, G., and van Impe. W. F. (2010). Diffusion of calcium chloride in a modified bentonite: Impact on osmotic efficiency and hydraulic conductivity. *Clays and Clay Minerals*, 58, 3, 351-363.

Shackelford, C.D. (2013). Membrane behavior of bentonite-based barriers: state of the art. *Proceedings of the International Symposium, ISSMGE TC 215, Coupled Phenomena in Environmental Geotechnics: From Theoretical and Experimental Research to Practical Applications*. Torino, Italy, M. Manassero, A. Dominijanni, S. Foti, and G. Musso, Eds., Taylor and Francis Group, London, UK, 45-60.

Shackelford, C. D. and Lee, J.-M. (2003). The destructive role of diffusion on clay membrane behavior. *Clays and Clay Minerals*, 51(2), 187-197.

Yeo, S.-S., Shackelford, C. D., and Evans, J. C. (2005). Membrane behavior of model soil-bentonite backfill mixtures. *Journal of Geotechnical and Geoenvironmental Engineering*, 131(4), 418-429.